DOI: 10.2478/eces-2026-0001 ECOL CHEM ENG S. 2026;33(1):7-20

Klaudia Barbara RACZAK[1], Abhilash VENKATESHAIAH[2], Mohammad GHEIBI[2]
Klaudiusz GRÜBEL[3], Edyta KUDLEK[4], Daniele SILVESTRI[2*], Vinod V.T. PADIL[5]
Miroslav ČERNÍK[2], Farshid GHANBARI[6], Kun-Yi Andrew LIN[7,8]
and Stanisław WACŁAWEK[2*]

COMPARATIVE STUDY OF FOUR UV-VIS LAMPS FOR PERSULPHATES-ACTIVATED DEGRADATION OF ACID BLUE 129

Abstract: Advanced oxidation processes employing sulphate radicals ($SO_4^{\bullet-}$) are effective techniques to degrade trace organic pollutants in wastewaters. Herein, $SO_4^{\bullet-}$ are generated from peroxymonosulphate (PMS) and peroxydisulphate (PDS) *via* UV-Vis activation for the degradation of Acid blue 129 (AB 129) dye. The activation was performed using four different UV-Vis lamps, TQ-150, HG-Z1, HG-Z2 and HG-Z3, which emit different electromagnetic radiation wavelengths. Degradation of AB 129 was performed at various conditions, including different oxidant concentrations. In order to evaluate the efficiency of the processes, the kinetic rate constant was calculated *via* a pseudo-first-order kinetics model. In addition, the detailed oxidative degradation pathway of AB 129 induced by $SO_4^{\bullet-}$ was determined for the first time to the best of our knowledge. Finally, the ECOSAR model indicates that the toxicity of the treated solution of Acid blue 129 initially increases and then decreases across daphnids, fish, and green algae during degradation.

Keywords: sulphate radical-advanced oxidation processes, peroxymonosulphate, peroxydisulphate, UV-Vis polychromatic lamps, Acid blue 129

[1] Faculty of Mechatronics, Informatics and Interdisciplinary Studies, Technical University of Liberec, 461 17 Liberec, Czech Republic, email: barbara.klaudia.raczak@tul.cz, mohammad.gheibi@tul.cz, ORCID: BKR 0009-0004-7928-0558, MG 0000-0003-1987-5790
[2] Institute for Nanomaterials, Advanced Technologies and Innovation, Technical University of Liberec, Studentská 1402/2, 46117 Liberec 1, Czech Republic, email: abhilashv4@gmail.com, daniele.silvestri@tul.cz, miroslav.cernik@tul.cz, stanislaw.waclawek@tul.cz, ORCID: AV 0000-0001-6121-9784, DS 0000-0002-5657-4818, MC 0000-0002-7554-020X, SW 0000-0002-8430-8269
[3] Department of Environmental Protection and Engineering, University of Bielsko-Biala, ul. Willowa 2, 43-309 Bielsko-Biala, Poland, email: kgrubel@ubb.edu.pl, ORCID: 0000-0002-0787-9324
[4] Department of Water and Wastewater Engineering, Silesian University of Technology, ul. S. Konarskiego 18, 44-100 Gliwice, Poland, email: edyta.kudlek@polsl.pl, ORCID: 0000-0003-0068-1996
[5] School of Nano Sciences, Central University of Gujarat, Kundhela-391107, Vadodara, Gujarat, India, email: vinod.padil@cug.ac.in, ORCID: 0000-0002-0816-526X
[6] Research Center for Environmental Contaminants (RCEC), Abadan University of Medical Sciences, Abadan, Iran, email: ghanbari.env@gmail.com, ORCID: 0000-0001-5599-3490
[7] Department of Environmental Engineering & Innovation and Development Center of Sustainable Agri-culture & Research Center of Sustainable Energy and Nanotechnology, National Chung Hsing University, 250 Kuo-Kuang Road, Taichung, Taiwan, email: linky@nchu.edu.tw, ORCID: 0000-0003-1058-3097
[8] Institute of Analytical and Environmental Sciences, National Tsing Hua University, Hsinchu, Taiwan
[*] Corresponding author: daniele.silvestri@tul.cz, stanislaw.waclawek@tul.cz

Introduction

Advanced oxidation processes (AOPs) are chemical processes that use highly reactive radical species to remediate pollutants in water [1-3]. AOPs are found to be effective in treating refractory contaminants resistant to other conventional techniques [4, 5]. They have been intensively investigated for the remediation of wastewaters generated from different industries [6], including food [7], petroleum refineries [8, 9] and textiles [10]. Traditionally, these processes usually employ highly reactive hydroxyl radicals ($HO^{\bullet}$) generated, e.g., from hydrogen peroxide (H_2O_2), to treat wastes and contaminants [11]. However, since $HO^{\bullet}$ has a very short half-life (~10^{-3} μs) and is often not economically feasible, alternative AOPs centred on the same strategy have been developed employing sulphate radicals ($SO_4^{\bullet-}$) [12]. These $SO_4^{\bullet-}$ have higher stability and longer half-life (~30 μs - 40 μs) as well as they typically favour electron transfer reactions as opposed to $HO^{\bullet}$, which react primarily *via* addition and H-abstraction [13, 14].

The peroxymonosulphate anion (PMS, HSO_5^-) and peroxydisulphate anion (PDS, $S_2O_8^{2-}$) are strong oxidants with a redox potential of 1.4 V and 2.01 V, respectively [15]. $SO_4^{\bullet-}$ can be generated by the catalytic activation of PMS or PDS by transition metals [16], electrolysis [17], radiolysis and UV irradiation [15] (Eqs. (1)-(4)) [18-20].

$$HSO_5^- + h\nu \rightarrow SO_4^{\bullet-} + HO^{\bullet} \quad (1)$$

$$HSO_5^- + e^- \rightarrow SO_4^{\bullet-} + HO^- \quad (2)$$

$$S_2O_8^{2-} + h\nu \rightarrow 2SO_4^{\bullet-} \quad (3)$$

$$S_2O_8^{2-} + e^- \rightarrow SO_4^{\bullet-} + SO_4^{2-} \quad (4)$$

When sulphate radicals are present in an aqueous medium at basic pH, they can produce $HO^{\bullet}$, as shown in equation [21]:

$$SO_4^{\bullet-} + OH^- \rightarrow HO^{\bullet} + SO_4^{2-} \quad (5)$$

Among the methods employed, UV light with a wavelength of 200 nm - 400 nm has been reported as an ecologically benign technique to generate sulphate radicals for degrading contaminants with high quantum efficiency and no concerns with metallic catalyst leakage [22]. Photoactivation of PMS and PDS can degrade pollutants efficiently as well as mineralise them under mild condition [23]. Furthermore, UV irradiation is often used in many water treatment procedures [24, 25], including disinfection, the addition of PMS and PDS, can result in a synergistic direct photodegradation and free radical oxidation [26]. UV-activated systems typically involve two steps in the degradation of pollutants [27]. UV irradiation could induce cleavage of chemical bonds, leading to the direct degradation of certain pollutants [28]. However, some contaminants are resistant to photolysis; therefore, direct photodegradation is insignificant [29]. On the other hand, in the indirect pathway, the energy from the UV light cleaves the peroxide bond of PMS/PDS, producing $SO_4^{\bullet-}$ [Eq. (3) for PDS] and both $SO_4^{\bullet-}$ and $HO^{\bullet}$ in the case of PMS [Eq. (1)] [15]. These $SO_4^{\bullet-}$ and $HO^{\bullet}$ obtained are strong oxidants capable of degrading numerous pollutants [30-32].

Li et al. developed a steady-state kinetic model to estimate the concentrations of reactive oxygen species (ROS) and their effect on the degradation of 4-chloro-3,5-dimethylphenol under various reaction conditions to gain insight into the reactive species involved in UV-activated persulfate system. The results indicated that the $SO_4^{\bullet-}$ was the predominant radical responsible for pollutant degradation, and that the overall process

efficiency strongly depends on the $SO_4^{\bullet-}$ concentration [33]. Further, in a UV/PDS system at pH 7, Liu et al. observed that $SO_4^{\bullet-}$ could be the primary active species in the degradation of oxytetracycline [34]. In addition to pH, UV activation of PMS/PDS is also strongly influenced by parameters such as the wavelength of the UV light utilised in the activation [35]. The UV electromagnetic spectrum, which is most widely described as 10 nm - 400 nm, may be segmented into many ranges as specified by ISO-21348. For the purposes of spectroscopy, the first classification is as follows: near UV: 300 nm - 400 nm; middle UV: 200 nm - 300 nm; far UV: 122 nm - 200 nm; extreme UV: 10 nm - 121 nm. Further classifications include UV-A: 315 nm - 400 nm; UV-B: 280 nm - 315 nm; UV-C: 100 nm - 280 nm. Due to its ability to photochemically activate numerous oxidant sources, short-wave UV-C has been used in several studies [36, 37]. Persulphate, hydrogen peroxide, and free chlorine have been activated using UV-C at a wavelength of 254 nm [38]. According to the observations made by Verma et al., UV light of wavelength 260 nm is more efficient than UV light with wavelengths of 270 nm, 280 nm and 290 nm in the activation of PMS to obtain a greater Anatoxin-a degradation [39]. The excitation energy at 260 nm is strong enough to promote cleavage of the peroxide bond of persulphates, resulting in the generation of $SO_4^{\bullet-}$ and $HO^{\bullet}$ and causing the degradation of the contaminant. Using shorter UV wavelengths to activate PMS or PDS may result in faster pollutant breakdown but a more significant energy cost. LEDs have recently been adopted as an emission source owing to their lower power consumption, faster warm-up time, durability, and ease of use [40]; nevertheless, UV LEDs' high cost and limited output power limit their application in large-scale treatment facilities [22]. Prolonged exposure to UV-C radiation can cause skin damage and potentially increase the risk of skin cancer. In contrast, long-wave ultraviolet radiation, such as UV-A, is less hazardous to biological tissues due to its lower frequency and photon energy. Nevertheless, both UV-A and UV-B radiation can be harnessed to promote environmentally friendly photochemical processes. Furthermore, utilising simulated solar radiation containing both UV and visible wavelengths can be beneficial for PMS/PDS activation, especially in the presence of an additional photocatalyst [35]. As a result, research focused on developing persulphate-based AOPs that are activated by simulated solar radiation has gained significant attention. This allows for more efficient utilisation of sunlight, making the process economically viable. However, for scientific reasons, lamps are easier to utilise and manage than solar light [41].

Dyes are chemical compounds used to impart colour to textiles, leather, paper and other materials. The wastewaters resulting from these industries contain residual dyes [42, 43]. When released into water bodies, they can affect the aesthetic quality and clarity of the water, while also harming aquatic life by reducing sunlight penetration, obstructing photosynthesis, and causing oxygen deficiency. Acid blue 129 (AB 129) is classified as an anthraquinone dye due to its characteristic chromophore, and it poses ecotoxic hazards and a risk of bioaccumulation in the environment [44]. Moreover, it can serve as a model pollutant for investigating the sulphate radical-advanced oxidation processes (SR-AOP) systems.

Recently, our group has reported on the degradation of AB 129 by a UV-Vis/PDS system [44], and determined the ecotoxicity of by-products produced by UV-Vis/PDS and UV-Vis/PMS [45]. Herein, we investigate the activation of PMS and PDS systems for the decolourisation of AB 129 using four different UV-Vis lamps. To the best of our knowledge, this is the first study employing four polychromatic lamps for PMS and PDS

activation under UV-Vis irradiation. In addition, an in-depth oxidative degradation pathway of AB 129 is reported for the first time. Finally, the toxicity of AB 129 and its by-products was analysed using the Ecological Structure Activity Relationships (ECOSAR) predictive model. The analysis included both acute and chronic toxicity categories for daphnid, fish, and green algae species [46]. The results obtained could help determine the most suitable polychromatic lamp for AB 129 degradation, considering both energy consumption and treatment efficiency.

Materials and methods

Chemicals

Oxone [triple salt, $KHSO_5 \cdot 0.5KHSO_4 \cdot 0.5K_2SO_4$ source of peroxymonosulphate (PMS)], sodium peroxydisulphate (PDS, persulphate, $Na_2S_2O_8$) and Acid blue (AB 129, $C_{23}H_{19}N_2NaO_5S$, 25 % dye content) were procured from Merck (Poznan, Poland). The studies were carried out with deionised water (18.2 MΩ·cm) acquired from the Polwater DL2-90 system (Labopol-Polwater, Krakow, Poland).

Analytical

The pH of the reaction mixture was measured using an inoLab®pH7310 (Weilheim, Germany) pH meter with SenTix®41 pH electrodes.

Hach Lange, DR 5000 UV-Vis spectrophotometer (Vancouver, WA, USA) was used to measure the visible spectrum of the samples within the 420 nm -750 nm wavelength range.

The analysis of the reaction by-product involved using GC-MS chromatography after a prior step of solid-phase extraction (SPE). The SPE was conducted using Supelclean™ ENVI-18 columns supplied by Sigma-Aldrich (Poznan, Poland). The chromatographic analysis was executed using the Agilent Technologies 7890 B GC-MS(EI) chromatograph (Santa Clara, USA). The specific protocols and methods for operating and analysing were outlined in a previously published study [45].

Decolourisation experiments

Decolourisation of AB 129 was performed according to our recently published article with a modified setup [44]. Briefly, in a 100 mL reactor, a 54.5 µM solution of AB 129 and different concentrations of PMS/PDS (0.625 mM, 1.25 mM, and 2.5 mM) were prepared. After that, the pH of the solutions was adjusted with 1 M NaOH or H_2SO_4 solution, and the prepared reactor was irradiated with UV-Vis light while being stirred constantly. UV-Vis lamps (medium-pressure mercury UV-Vis lamps; Heraeus, Hanau, Germany) model TQ-150, HG-Z1, HG-Z2, and HG-Z3 were used as UV-Vis sources in the study. The lamps were placed in a cooling jacket made of quartz glass (DURAN 50) and filled with recirculating tap water to ensure a constant temperature of (21 ± 1) °C. The effective arc length (electrode gap) of all evaluated UV-Vis lamps was 44 mm, while the optical path of light in all treated samples was < 2 cm. According to the data provided by the manufacturer, lamps in the cooling jacket emanate radiation with wavelength (λ_{exc}) as provided in Table 1. Each of these waves possesses different energy.

Table 1
Wavelength and flux of the emanating radiation from different lamps (values refer to the lamp used in the Duran 50 sleeve, values are given by the manufacturer)

Lamp	λ_{exc} [nm]	φ [W]
TQ-150	297, 302, 313, 334, 366, 390, 405/08, 436, 492, 546, 577/79	0.1, 0.5, 2.5, 0.4, 5.8, 0.1, 2.9, 3.6, 0.1, 4.6, 4.2
HG-Z1	297, 302, 313, 334, 352, 366, 378, 390, 405/08, 417, 436, 492, 535, 546, 577/79	0.4, 0.5, 1.9, 0.3, 0.4, 5.0, 0.6, 0.5, 4.1, 3.9, 3.9, 0.3, 0.3, 4.2, 4.2
HG-Z2	302, 313, 322, 334, 352, 366, 378, 405/08, 436, 536, 546, 577/79	0.1, 1.0, 0.7, 0.3, 5.6, 3.2, 3.8, 1.0, 2.1, 12.6, 2.4, 1.5
HG-Z3	297, 302, 313, 326, 334, 340, 346, 361, 366, 390, 405/08, 436, 467, 480, 492, 508, 546, 577/79	0.2, 0.5, 2.1, 0.5, 0.4, 0.5, 1.3, 2.5, 5.8, 0.4, 1.9, 4.4, 0.5, 1.5, 0.3, 1.9, 4.5, 4.6

ECOSAR simulation

In this study, ECOSAR 2.2 from the U.S. Environmental Protection Agency (EPA) was applied for ecotoxicological assessment [47]. All organic compounds were modelled in their neutral organic forms during the ECOSAR simulation. The exposure durations were set at 96 hours for fish, 48 hours for daphnids, and 96 hours for green algae. Toxicity was computed using LC50 for fish and daphnids, and EC50 for green algae. In the simulation processes, toxicity is assessed across four categories: 0-1 (very toxic), 1-10 (toxic), 10-100 (harmful), and over 100 (not harmful) [46].

Results

This study aimed to directly correlate the activation of PMS and PDS systems utilising four different lamps. Herein, we have used TQ-150, HG-Z1, HG-Z2 and HG-Z3 lamps as UV-Vis sources emanating radiations of different wavelengths (Table 1). Previous studies and our unpublished data indicate that PMS and PDS exhibit low reactivity without activation to generate reactive species for effective degradation [29]. Furthermore, AB 129 has been shown to be resistant to direct UV photolysis because the energy of photons with wavelengths spanning from 297 nm to 578 nm is insufficient to break down the dye molecule in the studied time [44]. The decolourisation of AB 129 dye was carried out at an initial concentration of 54.5 µM with three different dosages of oxidants: 0.625 mM, 1.25 mM and 2.5 mM exposed to irradiation for 15 min. The generation of $HO^{\bullet}$ *via* oxidation of water molecules can be disregarded, as this process is very slow ($6.6 \cdot 10^2\ M^{-1}\ s^{-1}$) and insignificant in the experiment's timescale [48]. The decolourisation of AB 129 *via* activation of PMS and PDS under different lamps and concentrations is given in Figure 1.

From the figure, it is evident that the degradation and the rate of degradation increase with the increase in the concentration of PMS and PDS. The increased generation of reactive oxygen species at higher oxidant concentrations is the cause of this phenomenon, which has been widely reported in the literature [49, 50]. Nevertheless, excessive PMS/PDS in the treatment of organic pollutants not only increases remediation costs but also converts sulphate radicals into sulphate anions [51], which affects the taste and quality of the drinking water [52]. Furthermore, higher PMS/PDS concentrations may inhibit the decolourisation owing to the self-scavenging of reactive oxidising species [53]. However, this behaviour was not seen at the concentrations used in this study, which is in agreement with our previous studies [44, 45].

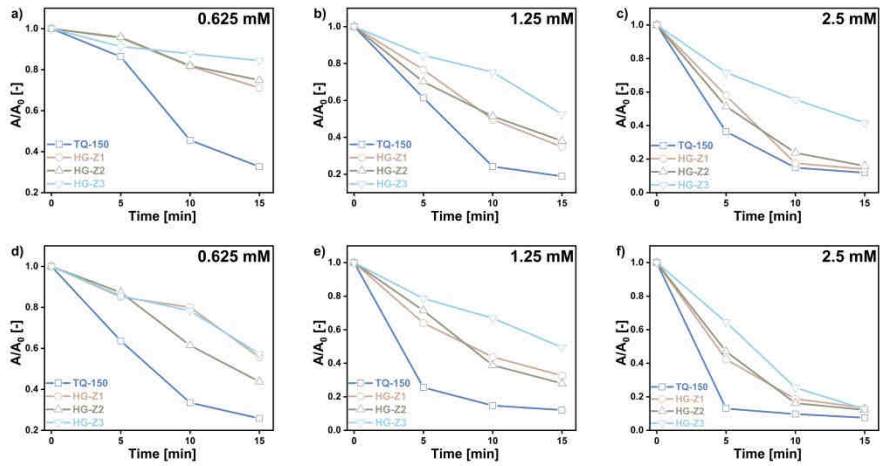

Fig. 1. Decolourisation of AB 129 by: a) - c) UV-Vis/PMS system and d) - f) UV-Vis/PDS system at different concentrations of oxidising agents

A pseudo-first-order kinetics model (Eq. (6)) was utilised to better analyse the decolourisation of AB 129 under UV-Vis activated PMS/PDS systems:

$$\ln(A_t/A_0) = -k_{app}t \tag{6}$$

where, A_0 and A_t are the absorbance of the solutions recorded at time 0 and time t [min], k_{app} is the apparent pseudo-first-order reaction rate constant.

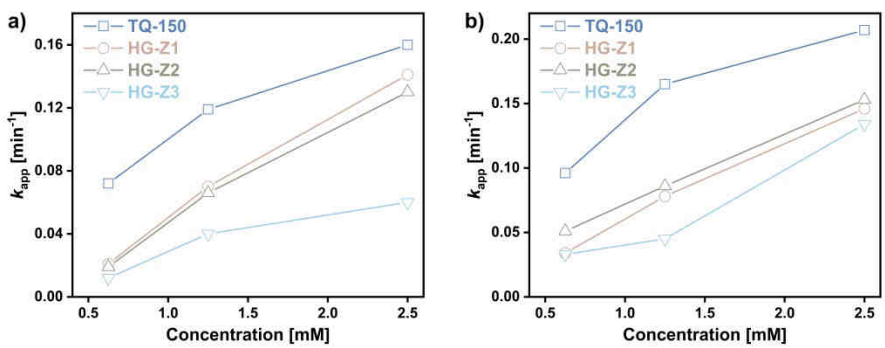

Fig. 2. Effect of the concentration of: a) UV-Vis/PMS and b) UV-Vis/PDS concentration on AB 129 decolourisation rate constant

Figure 2 shows that the UV-Vis/PDS system degrades AB 129 better than UV-Vis/PMS at the same oxidant concentration. This is because, for every mole of PDS, two moles of $SO_4^{\bullet-}$ are generated, while in the case of PMS, one mole of $SO_4^{\bullet-}$ and one mole of $HO^{\bullet}$ are generated. Owing to the different reaction mechanisms, the generated $HO^{\bullet}$ have a negligible effect on the AB 129 degradation [44]. $HO^{\bullet}$ reacts primarily *via* hydrogen

abstraction or addition, whereas $SO_4^{\bullet-}$ reacts mainly *via* electron transfer, making it highly reactive towards the -NH- group of AB 129 [44, 54]. This mechanism was investigated computationally, with the exact site of electron transfer determined by Waclawek [55].

The efficiency of different UV-Vis lamps in degrading AB 129 was evaluated at various oxidant concentrations (Fig. 3). With the UV-Vis/PMS system, TQ-150 performs the best at the end of 15 min at every concentration, followed by HG-Z1, HG-Z2 and HG-Z3. The efficiency of TQ-150 increases from ~67 %, ~81 % and ~88 % as the PMS dosage is increased from 0.625 mM, 1.25 mM and 2.5 mM, respectively. However, a significant increase in the degradation efficiency with concentration was observed in HG-Z1, and HG-Z2 lamps, whose efficiency leapt from ~29 % and ~24 % to ~86 % and ~84 % as the concentration of the oxidant was increased from 0.625 mM to 2.5 mM. HG-Z3 exhibited the lowest efficiency at all concentrations, with a ~58 % at 2.5 mM PMS concentration. Even in the case of the UV-Vis/PDS system, TQ-150 outperforms all the other lamps with an efficiency of ~74 %, ~88 %, and ~93 % at concentrations of 0.625 mM, 1.25 mM and 2.5 mM, respectively. At 2.5 mM PDS concentration, TQ-150 achieves a degradation of ~87 % within 5 min of the reaction time and thereafter increases only by ~5 % by the end of the reaction at 15 min. HG-Z2 exhibits next-best degradation efficiencies of ~56 %, ~72 % and ~88 % at PDS concentrations of 0.625 mM, 1.25 mM and 2.5 mM. Furthermore, at 2.5 mM PDS concentration, HG-Z2 degrades at a rate of 83 % within 5 minutes, similar to TQ-150. Even in this system, HG-Z3 has the lowest efficiency. However, at a PDS concentration of 2.5 mM, it has a similar performance as the other lamps, with a degradation efficiency of ~87 % at the end of 15 min.

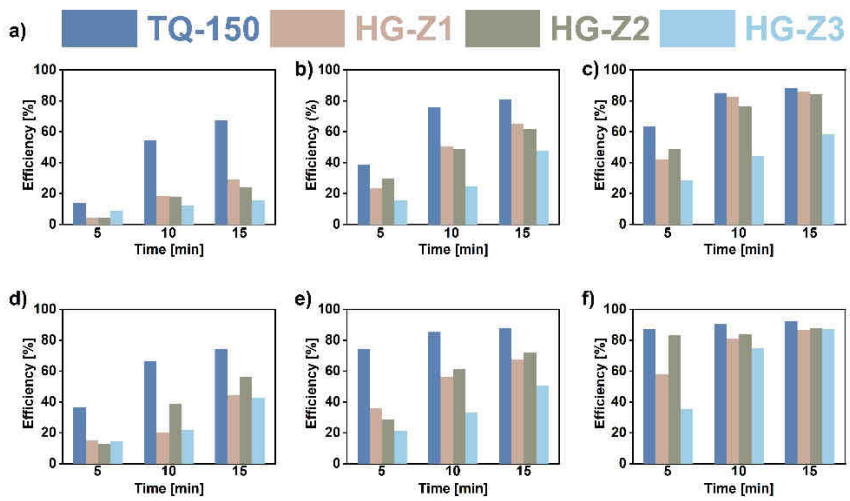

Fig. 3. Decolourisation efficiency of different UV-Vis lamps: a) UV-Vis/PMS/0.625 mM, b) UV-Vis/PMS/1.25 mM, c) UV-Vis/PMS/2.5 mM, d) UV-Vis/PDS/0.625 mM, e) UV-Vis/PDS/1.25 mM, and f) UV-Vis/PDS/2.5 mM

To further investigate the oxidative degradation process of the AB 129 dye, an in-depth analytical investigation was conducted using GC-MS chromatography. This allowed the identification and characterisation of the primary by-products formed during the

degradation process. Our study revealed, for the first time, the exact pathway presenting four major by-products: 1,2,4-trihydroxyanthraquinone (HA), 2,3-dihydroxynaphthoquinone (2,3-D), 5-methylpyrogallol (5-M), and p-hydroxytoluene (p-H). The formation of HA was observed in our previous paper [45], where an increase in UV-Vis absorbance at 540 nm (characteristic of red-coloured solutions) suggested the formation of a red dye intermediate during treatment. Although degradation pathways have been reported for structurally different Acid blue dyes such as Acid blue 1 [56], to the best of our knowledge, this is the first report on the oxidative degradation pathway of AB 129.

The determination of by-products is significant as it sheds light on the degradation pathway of AB 129 dye when subjected to UV/persulphates treatment. The determination of degradation by-products can help guide wastewater remediation by preventing the accumulation of more harmful substances of the parent compound [15].

For a comprehensive understanding of the findings, we have provided a detailed depiction of the degradation pathway in Figure 4, illustrating how the main by-products are formed. Additionally, Table 2 offers a thorough description of each of the identified compounds, including their chemical formula, molecular weight and top peaks.

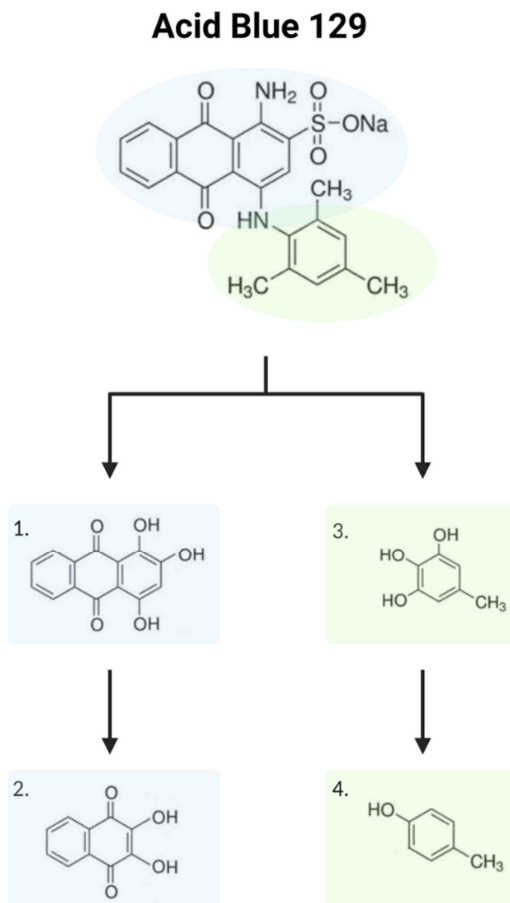

Fig. 4. Degradation pathway of AB 129

Table 2

Degradation products of AB 129

No.	Names	Formula	Molecular weight [g/mol]	m/z
1	1,2,4-trihydroxyanthraquinone	$C_{14}H_8O_5$	256.21	256, 228, 126, 115, 102
2	2,3-dihydroxynaphthoquinone	$C_{10}H_6O_4$	190.15	190, 162, 88
3	5-methylpyrogallol	$C_7H_8O_3$	140.14	140, 94
4	p-hydroxytoluene	C_7H_8O	108.14	108, 107, 90, 79, 77

The ecotoxicology assessment using the ECOSAR model for the AB 129 and its degradation products (Table 2) in both acute and chronic categories for three species-daphnids, fish, and green algae-is shown in Figure 5. According to Figure 5, in the acute categories for both daphnids and green algae, the toxicity level of AB 129 increases from harmful to toxic (due to HA formation). In the next step of the degradation, HA is converted to 2,3-D, which has a lower level of toxicity, making the end of this degradation pathway safe. In contrast, the other degradation pathway, indicates that the toxicity level increases from non-harmful 5-M to harmful p-H. However, the harmful level of p-H for daphnids is lower than that of AB 129. Therefore, for daphnids, it can be concluded that toxicity initially increases and then decreases, with the final degradation products having lower toxicity levels than the initial AB 129. Similarly, the experimental study performed by our group before [45] demonstrated that using a similar procedure as the present research, the toxicity level and effect of AB degradation initially increase and then decrease in the subsequent stages. In our previous study, the experimental ecotoxicological assessment was conducted for both *Lemna minor* and *Daphnia magna* (as part of the daphnid family) during the degradation of AB by a UV-activated persulphates oxidation process. The results showed a consistent pattern where the initial degradation products exhibited higher toxicity, which gradually diminished as the degradation progressed, ultimately resulting in less harmful end products [45]. This aligns with the findings of the current research, reinforcing the observation that the degradation pathway significantly influences the ecotoxicological outcomes for various species. In our previous study [45], the observed temporary increase in toxicity was attributed to the formation of toxic intermediates during persulphate-mediated dye degradation. However, after this study, it is quite clear that the “red by-product”-HA could be the main reason for the temporary toxicity increase. In the study of fish species, it is observed that in the first stage of degradation, the compound AB 129, initially categorised as non-harmful, breaks down into HA (a harmful substance) and 5-M (non-harmful). During the second stage of degradation, HA is further broken down into 2,3-D, which has the lowest toxicity level in the non-harmful category. Meanwhile, the non-harmful 5-M undergoes a transformation into p-H, which is harmful.

According to Figure 5, the chronic analysis demonstrated that in *Daphnia* species, AB 129, initially classified as toxic, degrades into HA and 5-M, which are categorised as very toxic and harmful, respectively. Following a similar pattern to the acute effects, HA, from the very toxic category, is further degraded into 2,3-D, classified as non-harmful, while 5-M, in the harmful category, is converted into p-H, which falls into the toxic category. Notably, the overall toxicity levels of the final degradation products (2,3-D and p-H) are lower than the initial toxicity level of AB. This indicates a net reduction in toxicity through the degradation process. In the fish species category, the

degradation trends are similar to those observed in daphnids. However, a key difference is that HA is categorised as toxic rather than very toxic. Despite this variation, the final products, 2,3-D and p-H, also exhibit lower toxicity levels compared to the original AB compound. The green algae chronic assessment demonstrated that AB at harmful levels is divided into HA (toxic) and 5-M (harmful) categories. HA is then converted to 2,3-D (with a concentration threshold of 184 mg/L) in the not-harmful category, while 5-M is converted to p-H in the toxic category.

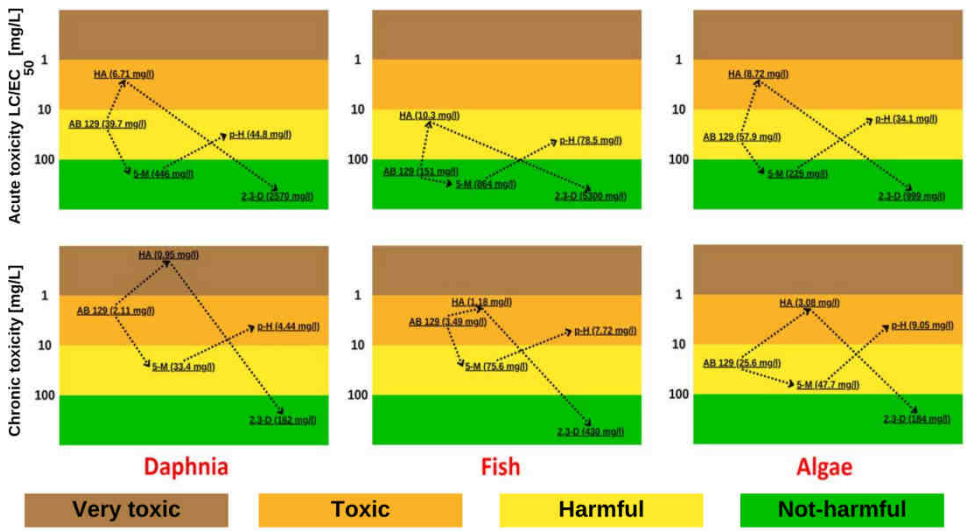

Fig. 5. The results of ecotoxicological simulation of AB 129 along the determined pathway in acute and chronic categories

One of the biggest concerns with SR-AOP is the production of large amounts of sulphate ions. To protect aquatic life, sulphate ions should be less than 500 mg/L [57]. However, maintaining this level during remediation using PDS or PMS to effectively remove contaminants might be challenging. Combining SR-AOP with other treatment methods, such as membrane filtration, may be one way to reduce sulphate ions [58]. In addition, the need for specialised UV equipment and accurate control of operational parameters increases the complexity of the purification process, which can increase maintenance requirements and operational costs [59]. This study also presents certain limitations, as it was conducted under controlled laboratory conditions that may not fully reflect the complexity of natural water matrices. The influence of inherent water constituents on sulphate radical generation and pollutant degradation was not extensively investigated. Although this work included a toxicological assessment, future research should focus on performing more comprehensive toxicological evaluations, validating these processes in real wastewater environments, and assessing their scalability to ensure both environmental safety and practical feasibility.

Conclusion

- Degradation and decolourisation of AB 129 were achieved using PMS and PDS activated by UV-Vis lamps.
- UV-Vis/PDS system was more efficient than UV-Vis/PMS, possibly due to higher sulphate radical generation.
- Four main by-products were identified: 1,2,4-trihydroxyanthraquinone, 2,3-dihydroxynaphthoquinone, 5-methylpyrogallol, and p-hydroxytoluene.
- Toxicity analysis revealed that the treatment by-products were initially more toxic as intermediates, but the final products were less toxic than AB 129, confirming the effectiveness of the detoxification process and results obtained in our previous study [45].

Acknowledgements

The results presented herein were supported by Project LL2501, “Hydrated electron: the alchemist stone of water treatment CZ”, funded by the Ministry of Education, Youth and Sports of the Czech Republic within the ERC CZ programme as well as by the Ministry of Education, Youth and Sports of the Czech Republic and the European Union European Structural and Investment Funds in the frames of Operational Programme Research, Development and Education - project Hybrid Materials for Hierarchical Structures (HyHi, Reg. No. CZ.02.1.01/0.0/0.0/16_019/0000843).

References

[1] Gu X, Lu S, Qiu Z, Sui Q, Miao Z, Lin K, et al. Comparison of photodegradation performance of 1,1,1-trichloroethane in aqueous solution with the addition of H_2O_2 or $S_2O_8^{2-}$ oxidants. Industrial Eng Chem Res. 2012;51:7196-204. DOI: 10.1021/ie202769d.

[2] Iqbal J, Shah NS, Ali Khan J, Habila MA, Boczkaj G, Shad A, et al. Bimetallic Bi/Cu0-catalyzed persulfate-based advanced oxidation processes towards clofibric acid degradation in wastewater. Water Resources Industry. 2023;30:100226. DOI: 10.1016/j.wri.2023.100226.

[3] Sui C, Nie Z, Liu H, Boczkaj G, Liu W, Kong L, et al. Singlet oxygen-dominated peroxymonosulfate activation by layered crednerite for organic pollutants degradation in high salinity wastewater. J Environ Sci. 2024;135:86-96. DOI: 10.1016/j.jes.2023.01.010.

[4] Jiang P, Li X-W, Wang J-A, Zhou X-L. Kinetic and mechanism studies on the photodegradation of cold-rolling emulsion wastewater by the UV/H_2O_2 process. Industrial Eng Chem Res. 2021;60:8073-84. DOI: 10.1021/acs.iecr.1c00835.

[5] Mohod AV, Momotko M, Shah NS, Marchel M, Imran M, Kong L, et al. Degradation of Rhodamine dyes by Advanced Oxidation Processes (AOPs) - Focus on cavitation and photocatalysis - A critical review. Water Resources Industry. 2023;30:100220. DOI: 10.1016/j.wri.2023.100220.

[6] Jiang P, Zhou J, Zhou Q, Xiang F, Wang J-A, Zhou X-L. Efficient degradation of high-concentration benzotriazole wastewater via UV/H_2O_2/O_3 operation: Degradation mechanism, toxicological evaluation, and economic analysis. Industrial Eng Chem Res. 2022;61:16431-44. DOI: 10.1021/acs.iecr.2c02596.

[7] Ioannou LA, Puma GL, Fatta-Kassinos D. Treatment of winery wastewater by physicochemical, biological and advanced processes: A review. J Hazardous Materials. 2015;286:343-68. DOI: 10.1016/j.jhazmat.2014.12.043.

[8] Diya’Uddeen BH, Daud WMAW, Abdul Aziz AR. Treatment technologies for petroleum refinery effluents: A review. Process Safety Environ Protection. 2011;89:95-105. DOI: 10.1016/j.psep.2010.11.003.

[9] Fakhru’l-Razi A, Pendashteh A, Abdullah LC, Biak DRA, Madaeni SS, Abidin ZZ. Review of technologies for oil and gas produced water treatment. J Hazard Materials. 2009;170:530-51. DOI: 10.1016/j.jhazmat.2009.05.044.

[10] Asghar A, Raman AAA, Daud WMAW. Advanced oxidation processes for in-situ production of hydrogen peroxide/hydroxyl radical for textile wastewater treatment: A review. J Cleaner Prod. 2015;87:826-38. DOI: 10.1016/j.jclepro.2014.09.010.
[11] Jung J, Kim J, Yoon S, Kumar Reddy PA, Hwang Y, Bae S. The role of Fe dissolution in olivine-hydroxylamine-induced Fenton reaction for enhanced oxidative degradation of organic pollutant. Chemosphere. 2022;306:135557. DOI: 10.1016/j.chemosphere.2022.135557.
[12] Raczak KB, Silvestri D, Myslik P, Marton P, Salava M, Padil VVT, et al. Sulfate radical-mediated degradation of vancomycin: Kinetics, mechanism, and toxicity evaluation. Separation Purif Technol. 2025;379:134935. DOI: 10.1016/j.seppur.2025.134935.
[13] Rastogi A, Al-Abed SR, Dionysiou DD. Sulfate radical-based ferrous-peroxymonosulfate oxidative system for PCBs degradation in aqueous and sediment systems. Appl Catalysis B: Environ. 2009;85:171-9. DOI: 10.1016/j.apcatb.2008.07.010.
[14] Wu J, Zou J, Li S, Tang C, Wu Z, He L, et al. Hydrogen peroxide enhanced Cu(II)/peroxymonosulfate system for naproxen degradation in natural water matrix and simultaneously reduced the formation potential of halogenated by-products. Chem Eng J. 2024;494:152979. DOI: 10.1016/j.cej.2024.152979.
[15] Wacławek S, Lutze HV, Grübel K, Padil VVT, Černík M, Dionysiou DD. Chemistry of persulfates in water and wastewater treatment: A review. Chem Eng J. 2017;330:44-62. DOI: 10.1016/j.cej.2017.07.132.
[16] Socha B, Silvestri D, Grübel K, Padil VVT, Dudziak M, Ghanbari F, et al. Activation of peroxydisulfate by bimetallic nano zero-valent iron for waste-activated sludge disintegration. Catalysts. 2022;12:590. DOI: 10.3390/CATAL12060590.
[17] Khavari Kashani MR, Wang Q, Khatebasreh M, Li X, Sheikh Asadi AM, Boczkaj G, et al. Sequential treatment of landfill leachate by electrocoagulation/aeration, PMS/ZVI/UV and electro-Fenton: Performance, biodegradability and toxicity studies. J Environ Manag. 2023;338:117781. DOI: 10.1016/j.jenvman.2023.117781.
[18] Waldemer RH, Tratnyek PG, Johnson RL, Nurmi JT. Oxidation of chlorinated ethenes by heat-activated persulfate: Kinetics and products. Environ Sci Technol. 2007;41:1010-5. DOI: 10.1021/es062237m.
[19] Luo C, Ma J, Jiang J, Liu Y, Song Y, Yang Y, et al. Simulation and comparative study on the oxidation kinetics of atrazine by UV/H_2O_2, UV/HSO_5^- and UV/$S_2O_8^{2-}$. Water Res. 2015;80:99-108. DOI: 10.1016/j.watres.2015.05.019.
[20] Xiao G, Xu T, Faheem M, Xi Y, Zhou T, Moryani HT, et al. Evolution of singlet oxygen by activating peroxydisulfate and peroxymonosulfate: A review. Int J Environ Res Public Health. 2021;18:3344. DOI: 10.3390/ijerph18073344.
[21] Wacławek S, Lutze HV, Sharma VK, Xiao R, Dionysiou DD. Revisit the alkaline activation of peroxydisulfate and peroxymonosulfate. Current Opinion Chem Eng. 2022;37:100854. DOI: 10.1016/j.coche.2022.100854.
[22] Yang J, Zhu M, Dionysiou DD. What is the role of light in persulfate-based advanced oxidation for water treatment? Water Res. 2021;189:116627. DOI: 10.1016/j.watres.2020.116627.
[23] Yang Q, Ma Y, Chen F, Yao F, Sun J, Wang S, et al. Recent advances in photo-activated sulfate radical-advanced oxidation process (SR-AOP) for refractory organic pollutants removal in water. Chem Eng J. 2019;378:122149. DOI: 10.1016/j.cej.2019.122149.
[24] Iervolino G, Zammit I, Vaiano V, Rizzo L. Limitations and prospects for wastewater treatment by UV and visible-light-active heterogeneous photocatalysis: A critical review. Heterog Photocatalysis: Recent Adv. 2020;225-64. DOI: 10.1007/978-3-030-49492-6_7.
[25] Vaiano V, Jaramillo-Paez CA, Matarangolo M, Navío JA, del Carmen Hidalgo M. UV and visible-light driven photocatalytic removal of caffeine using ZnO modified with different noble metals (Pt, Ag and Au). Materials Res Bull. 2019;112:251-60. DOI: 10.1016/j.materresbull.2018.12.034.
[26] Díez AM, Sanromán MA, Pazos M. New approaches on the agrochemicals degradation by UV oxidation processes. Chem Eng J. 2019;376:120026. DOI: 10.1016/j.cej.2018.09.187.
[27] Guerra-Rodríguez S, Ribeiro ARL, Ribeiro RS, Rodríguez E, Silva AMT, Rodríguez-Chueca J. UV-A activation of peroxymonosulfate for the removal of micropollutants from secondary treated wastewater. Sci Total Environ. 2021;770:145299. DOI: 10.1016/j.scitotenv.2021.145299.
[28] Zhang R, Sun P, Boyer TH, Zhao L, Huang CH. Degradation of pharmaceuticals and metabolite in synthetic human urine by UV, UV/H_2O_2, and UV/PDS. Environ Sci Technol. 2015;49:3056-66. DOI: 10.1021/es504799n.
[29] Wang J, Wang S. Activation of persulfate (PS) and peroxymonosulfate (PMS) and application for the degradation of emerging contaminants. Chem Eng J. 2018;334:1502-17. DOI: 10.1016/j.cej.2017.11.059.
[30] Lee D, Kim S, Tang K, Kim T-H, Kim SD, Park Y, et al. Utilization of iron-based waste derived from the biogas desulfurization process as an economic catalyst for tetracycline oxidation in water. Environmental Technol Innov. 2023;29:103006. DOI: 10.1016/j.eti.2023.103006.

[31] Lee D, Kim S, Tang K, De Volder M, Hwang Y. Oxidative degradation of tetracycline by magnetite and persulfate: performance, water matrix effect, and reaction mechanism. Nanomaterials. 2021;11:2292. DOI: 10.3390/nano11092292.
[32] Luo C, Jiang J, Ma J, Pang S, Liu Y, Song Y, et al. Oxidation of the odorous compound 2,4,6-trichloroanisole by UV activated persulfate: Kinetics, products, and pathways. Water Res. 2016;96:12-21. DOI: 10.1016/j.watres.2016.03.039.
[33] Li W, Guo H, Wang C, Zhang Y, Cheng X, Wang J, et al. ROS reevaluation for degradation of 4-chloro-3,5-dimethylphenol (PCMX) by UV and UV/persulfate processes in the water: Kinetics, mechanism, DFT studies and toxicity evolution. Chem Eng J. 2020;390:124610. DOI: 10.1016/j.cej.2020.124610.
[34] Liu Y, He X, Fu Y, Dionysiou DD. Kinetics and mechanism investigation on the destruction of oxytetracycline by UV-254 nm activation of persulfate. J Hazard Materials. 2016;305:229-39. DOI: 10.1016/j.jhazmat.2015.11.043.
[35] Song T, Li G, Hu R, Liu Y, Liu H, Gao Y. Degradation of antibiotics via UV-activated peroxodisulfate or peroxymonosulfate: A review. Catalysts. 2022;12:1025. DOI: 10.3390/catal12091025.
[36] Xu M, Deng J, Cai A, Ma X, Li J, Li Q, et al. Comparison of UVC and UVC/persulfate processes for tetracycline removal in water. Chem Eng J. 2020;384:123320. DOI: 10.1016/j.cej.2019.123320.
[37] Dan J, Wang Q, Mu K, Rao P, Dong L, Zhang X, et al. Degradation of sulfachloropyridazine by UV-C/persulfate: kinetics, key factors, degradation pathway. Environmental Science: Water Res Technol. 2020;6:2510-20. DOI: 10.1039/D0EW00239A.
[38] Sánchez-Montes I, Wachter N, Silva BF, Aquino JM. Comparison of UVC-based advanced oxidation processes in the mineralization of bisphenol A: Identification of oxidation by products and toxicity evaluation. Chem Eng J. 2020;386:123986. DOI: 10.1016/j.cej.2019.123986.
[39] Verma S, Nakamura S, Sillanpää M. Application of UV-C LED activated PMS for the degradation of anatoxin-a. Chem Eng J. 2016;284:122-9. DOI: 10.1016/j.cej.2015.08.095.
[40] Rasoulifard MH, Fazli M, Eskandarian MR. Performance of the light-emitting-diodes in a continuous photoreactor for degradation of Direct Red 23 using UV-LED/$S_2O_8^{2-}$ process. J Industrial Eng Chem. 2015;24:121-6. DOI: 10.1016/j.jiec.2014.09.018.
[41] Gabet A, Métivier H, de Brauer C, Mailhot G, Brigante M. Hydrogen peroxide and persulfate activation using UVA-UVB radiation: Degradation of estrogenic compounds and application in sewage treatment plant waters. J Hazard Materials. 2021;405:124693. DOI: 10.1016/j.jhazmat.2020.124693.
[42] Liugė M, Paliulis D, Kumpienė J, Paulauskienė T. Removal of textile dyes from water using cellulose aerogel. Ecol Chem Eng S. 2024;31:49-62. DOI: 10.2478/eces-2024-0004.
[43] Zein R, Wulandari S, Ramadhani P, Deswati D. Utilisation of shrimp shell as a low-cost biosorbent for the adsorption of methylene blue dyes. Ecol Chem Eng S. 2024;31:63-73. DOI: 10.2478/eces-2024-0005.
[44] Krawczyk K, Wacławek S, Kudlek E, Silvestri D, Kukulski T, Grübel K, et al. UV-catalyzed persulfate oxidation of an anthraquinone based dye. Catalysts. 2020;10:456. DOI: 10.3390/catal10040456.
[45] Ramakrishnan RK, Venkateshaiah A, Grübel K, Kudlek E, Silvestri D, Padil VVT, et al. UV-activated persulfates oxidation of anthraquinone dye: Kinetics and ecotoxicological assessment. Environ Res. 2023;229:115910. DOI: 10.1016/j.envres.2023.115910.
[46] Yaghoot-Nezhad A, Wacławek S, Madihi-Bidgoli S, Hassani A, Lin K-YA, Ghanbari F. Heterogeneous photocatalytic activation of electrogenerated chlorine for the production of reactive oxygen and chlorine species: A new approach for Bisphenol A degradation in saline wastewater. J Hazard Materials. 2023;445:130626. DOI: 10.1016/j.jhazmat.2022.130626.
[47] US EPA O. Ecological Structure Activity Relationships (ECOSAR) Predictive Model 2015. Available from: https://www.epa.gov/tsca-screening-tools/ecological-structure-activity-relationships-ecosar-predictive-model (accessed August 8, 2025).
[48] Crincoli KR, Green C, Huling SG. Sulfate radical scavenging by mineral surfaces in persulfate-driven oxidation systems: Reaction rate constants and implications. Environ Sci Technol. 2020;54:1955-62. DOI: 10.1021/acs.est.9b06442.
[49] Lu X, Shao Y, Gao N, Chen J, Zhang Y, Xiang H, et al. Degradation of diclofenac by UV-activated persulfate process: Kinetic studies, degradation pathways and toxicity assessments. Ecotoxicol Environ Safety. 2017;141:139-47. DOI: 10.1016/j.ecoenv.2017.03.022.
[50] Bekris L, Frontistis Z, Trakakis G, Sygellou L, Galiotis C, Mantzavinos D. Graphene: A new activator of sodium persulfate for the advanced oxidation of parabens in water. Water Res. 2017;126:111-21. DOI: 10.1016/j.watres.2017.09.020.
[51] Long Y, Wu Z, Ding X, Chen J, Shen D, Shentu J, et al. Potential risks of organic contaminated soil after persulfate remediation: Harmful gaseous sulfur release. J Environ Sci. 2024;135:1-9. DOI: 10.1016/j.jes.2023.01.008.

[52] Burlingame GA, Dietrich AM, Whelton AJ. Understanding the basics of tap water taste. J AWWA. 2007;99:100-11. DOI: 10.1002/j.1551-8833.2007.tb07930.x.
[53] Ghanbari F, Moradi M. Application of peroxymonosulfate and its activation methods for degradation of environmental organic pollutants: Review. Chem Eng J. 2017;310:41-62. DOI: 10.1016/j.cej.2016.10.064.
[54] Ghauch A, Baalbaki A, Amasha M, El Asmar R, Tantawi O. Contribution of persulfate in UV-254 nm activated systems for complete degradation of chloramphenicol antibiotic in water. Chem Eng J. 2017;317:1012-25. DOI: 10.1016/j.cej.2017.02.133.
[55] Wacławek S. Do we still need a laboratory to study advanced oxidation processes? A review of the modelling of radical reactions used for water treatment. Ecol Chem Eng S. 2021;28:11-28. DOI: 10.2478/ECES-2021-0002.
[56] Chen C-C, Fan H-J, Jan J-L. Degradation pathways and efficiencies of Acid Blue 1 by photocatalytic reaction with ZnO nanopowder. J Physical Chem C. 2008;112:11962-72. DOI: 10.1021/jp801027r.
[57] Duan X, Yang S, Wacławek S, Fang G, Xiao R, Dionysiou DD. Limitations and prospects of sulfate-radical based advanced oxidation processes. J Environ Chem Eng. 2020;8:103849. DOI: 10.1016/J.JECE.2020.103849.
[58] Yan H, Lai C, Wang D, Liu S, Li X, Zhou X, et al. In situ chemical oxidation: peroxide or persulfate coupled with membrane technology for wastewater treatment. J Materials Chem A. 2021;9:11944-60. DOI: 10.1039/D1TA01063H.
[59] Norzaee S, Bazrafshan E, Djahed B, Kord Mostafapour F, Khaksefidi R. UV Activation of persulfate for removal of penicillin G antibiotics in aqueous solution. Scientific World J. 2017;2017. DOI: 10.1155/2017/3519487.